Noncontact inspection technique for electrical failures in semiconductor devices using a laser terahertz emission microscope

Masatsugu Yamashita,[1,a)] Chiko Otani,[1] Kodo Kawase,[1,2] Kiyoshi Nikawa,[3] and Masayoshi Tonouchi[4]
[1]*RIKEN Sendai, 519-1399 Aoba, Aramaki, Aoba-ku, Sendai, Miyagi 980-0845, Japan*
[2]*EcoTopia Science Institute, Nagoya University, Furocho, Chikusa-ku, Nagoya 464-8603, Japan*
[3]*NEC Electronics, 1753 Shimonumabe, Nakahara-ku, Kawasaki 211-8668, Japan*
[4]*Institute of Laser Engineering, Osaka University, 2-6 Yamadaoka, Suita, Osaka 565-0871, Japan*

(Received 8 June 2008; accepted 9 July 2008; published online 31 July 2008)

We have proposed and demonstrated a novel technique for the noncontact inspection of electrical failures in semiconductor devices using a laser terahertz emission microscope. It was found that the waveforms of the terahertz pulses, emitted by exciting *p-n* junctions in semiconductor circuits with focused ultrafast laser pulses, depend on the interconnection structures of the circuits. We successfully distinguished damaged silicon metal-oxide-semiconductor field effect transistor circuits with disconnected wires from normal ones by comparing the images of terahertz emission amplitudes between a normal chip and a defective one. © *2008 American Institute of Physics*. [DOI: 10.1063/1.2965810]

The terahertz spectral range has been an active field of research for the past two decades. This research has been stimulated by the development of ultrafast lasers and of the gated terahertz emission and detection techniques that facilitated various applications such as terahertz spectroscopy and imaging.[1,2] In Refs. 3–5, we proposed and demonstrated the laser terahertz emission microscope (LTEM) as a novel tool for inspection and failure analysis of large scale integration circuits (LSICs) with bias voltages. For LSIC inspection, LTEM acquires terahertz emission images generated by photoconductive switching in a LSIC by scanning it with ultrafast laser pulses. The electrical failures such as a wire disconnection can be identified as the change in the terahertz emission images induced by the change in the electric field distribution in the circuits.

Several LSIC testing techniques, including the infrared optical beam induced resistance change, the photoemission microscope, the electron beam testing, etc., are used in practice to inspect and to localize electrical failures in LSICs.[6–8] However, these techniques require the electrical contacts between the chip and the outside equipment to apply the bias voltage to or to read the electrical signal from the LSIC. On the other hand, the pattern defect in-line inspection methods do not require electrical contacts but the defects they can find are not always the potential causes of electrical failures. Therefore, inspection techniques for electrical failures in LSICs without electrical contact are strongly required not only for the acceleration of LSIC research and development but also for the improvement of the quality and reliability. Laser-superconducting quantum interfence device (SQUID) microscope, which measures the magnetic field of laser-induced photocurrent in circuits, has been proposed and studied to improve this situation.[9]

In this letter, we applied the LTEM technique for the noncontact inspection of silicon metal-oxide-semiconductor field effect transistor (Si-MOSFET) circuits without any electrical contacts and successfully distinguished between damaged Si-MOSFET circuits and normal ones. This result is the first experimental step for the inspection of LSIC chip without any electrical contacts. The expected coverage of this noncontact method is compared to that of conventional methods in Fig. 1.

Terahertz pulses can be generated from nonbiased Si-MOSFETs by exciting *p-n* junctions with ultrafast laser pulses. The electric fields of the depletion layers in *p-n* junctions accelerate the photoexcited carriers and the transient photocurrent generates terahertz pulses. Here, the waveforms of terahertz pulses depend on the interconnection structure near the *p-n* junctions because photocurrent flow into the interconnection lines and the interconnection line works as a terahertz antenna. Therefore, it is expected that when there are defects in the circuit wiring, the change could be seen in the terahertz emission images.

Figure 2(a) shows the schematic diagram of the experimental setup. A mode-locked Ti:sapphire laser (76 MHz repetition rate, 800 nm wavelength, and 130 fs pulse duration) was used to both generate and detect the terahertz pulses

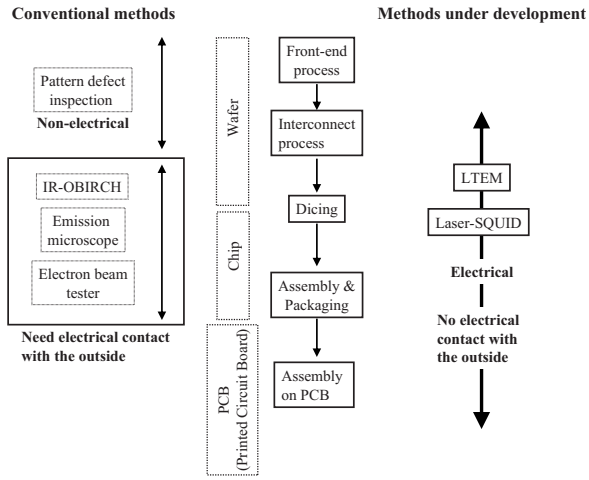

FIG. 1. Position of the LTEM among other nondestructive LSIC testing methods.

a)Electronic mail: m-yama@riken.jp.

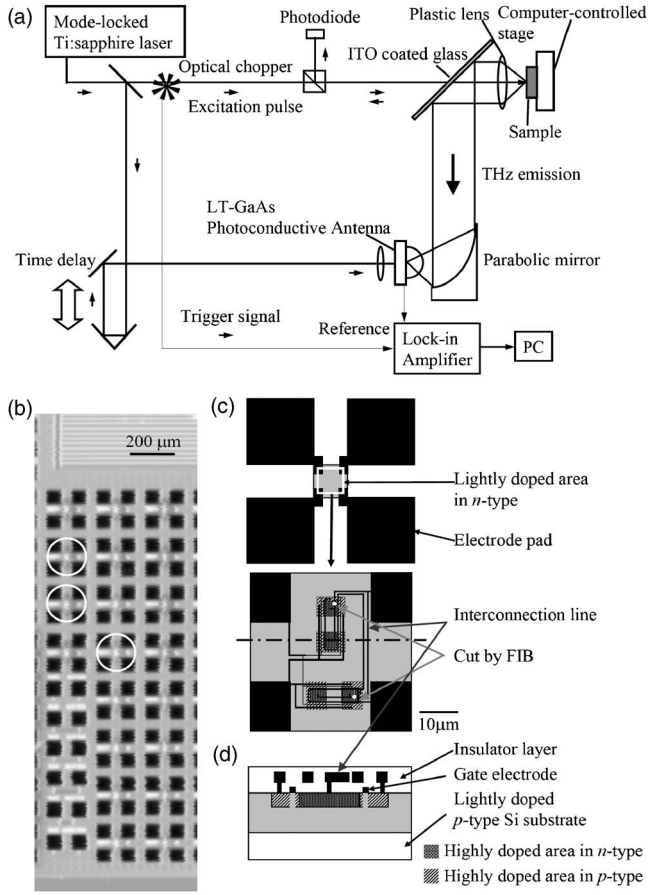

FIG. 2. (a) Experimental setup of LTEM for LSIC inspection. (b) The laser reflection image of the Si-MOSFET chip. The test circuits circled in white have lines damaged by cutting them by FIB. (c) Schematic of the *p*-MOSFET circuit structure indicated by the white circles in (b). (d) A cross section of the *p*-MOSFET circuit in (c).

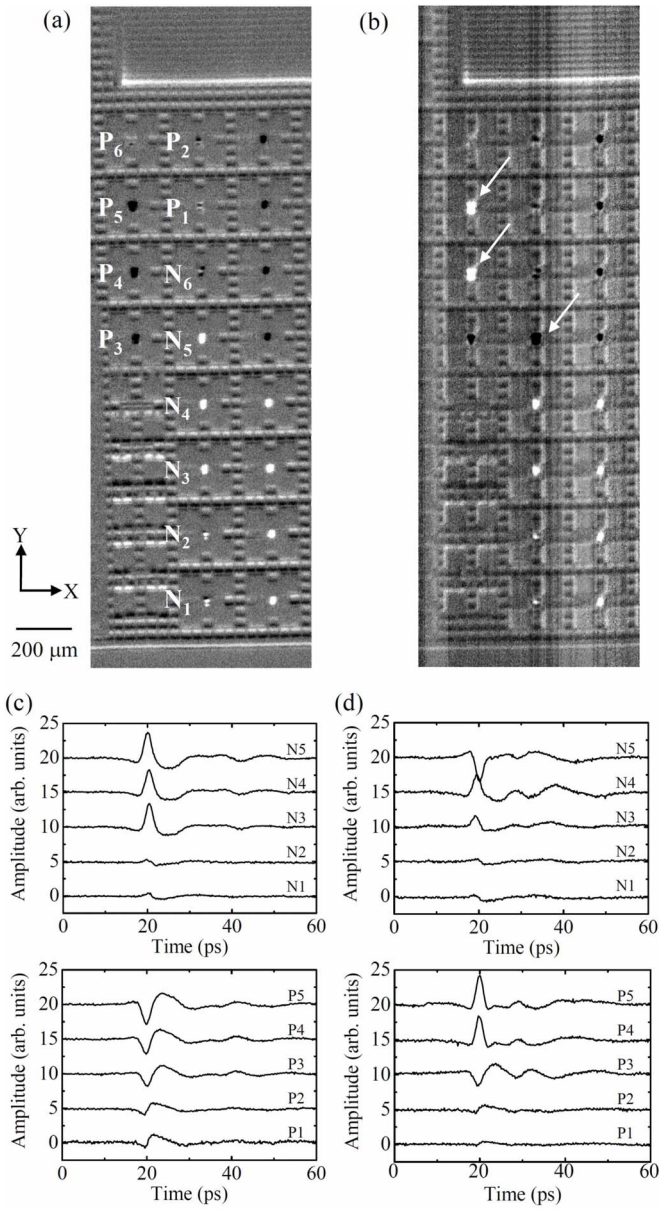

FIG. 3. Comparison of the terahertz emission images and waveforms between a normal chip and a defective one: [(a) and (b)] the terahertz emission images from the normal chip and the defective one, respectively. White and black areas show positive and negative amplitude of terahertz emissions from *p-n* junctions surrounded by four electrode pads each. The white arrows indicate three damaged MOSFET circuits in the defective chip; [(c) and (d)] the terahertz emission waveforms from the normal chip and the defective one, respectively.

from the sample. The excitation laser pulses were focused onto the sample surface by an aspherical plastic lens (Tsurupica Pax Co.), and the terahertz pulses emitted backward were collected by the same lens. The collimated terahertz emission was reflected by an indium-tin oxide thin film coated glass substrate and focused onto a low-temperature-grown GaAs photoconductive switch. The temporal waveforms of the terahertz emission were measured by scanning the time delay for trigger pulses, and the terahertz emission images were obtained by moving the sample two dimensionally and fixing the time delay stage at a position around the peak of the terahertz waveform. Scanning laser reflection images were also acquired at the same time.

Figure 2(b) shows the laser reflection image of the MOSFET circuit chip including a series of *n*-channel (N_1-N_6) and *p*-channel (P_1-P_6) MOSFETs (*n*-MOSFETs and *p*-MOSFETs), and (c) shows a magnified schematic illustration of a *p*-channel MOSFET circuit in the chip. The main difference in the circuit structure between N_1-N_6 and P_1-P_6 is the position of the gate electrode. For comparison, we prepared a defective chip including three MOSFET circuits [circled in Fig. 2(b)] that were damaged by cutting lines near the *p-n* junctions using a focused ion beam (FIB).

Figures 3(a) and 3(b) show the terahertz emission images of a normal and a defective MOSFET circuit chip, respectively. To avoid the laser-induced damage on the sample, the terahertz emission images were acquired with an average excitation laser power below 30 mW (160 $\mu J/cm^2$) measured after the optical chopper. It is seen that the sign of the terahertz emission amplitude depends on the direction of the electric field in the depletion layer of the *p-n* junctions. Figure 3(c) shows the waveforms of the terahertz emissions from MOSFET circuits in the normal chip. The polarity of the terahertz emission waveforms from the *p*-MOSFET circuits is reversed compared to those from the *n*-MOSFET ones, which is in agreement with the contrast of the terahertz emission image in Fig. 3(a). The spatial resolution of the images in Figs. 3(a) and 3(b) is approximately 25 μm, which depends on the laser spot size and covers the area of the *p-n* junctions in the circuit, and the detected polarization of terahertz emission was in the *Y* direction. The terahertz emission

amplitudes are different between the circuits N_1-N_5 and P_1-P_5. In circuits N_6 and P_6, the interconnection lines from the electrode pad are not connected to the *p-n* junctions and their terahertz emission signals are considerably small compared to other circuits. These features can also be seen in the terahertz emission waveforms, which indicate that the interconnection lines work as an antenna, and terahertz emission amplitudes and waveforms depend on the interconnection structure connected to the photoexcited *p-n* junctions.

By comparing Figs. 3(a) and 3(b), one can see the polarity change in the terahertz emission amplitude between normal circuits and damaged ones. Figure 3(d) shows the terahertz emission waveforms from the defective chip. The terahertz emission waveforms from the damaged circuits also change compared to those from normal ones in Fig. 3(c). We consider that this terahertz waveform changed between normal and damaged circuits can be attributed to the change in the interconnection structure introduced by cutting the interconnections. This result indicates that the LTEM can be used for the inspection of defects of interconnection structure in semiconductor devices without any electrical contacts between the chip and outside equipment.

In summary, a noncontact inspection technique for LSICs, without any electrical contacts, using LTEM was proposed and its first experimental results were obtained on test circuits composed of Si-MOSFETs as a sample. It was found that the terahertz emission waveforms from Si-MOSFETs are affected by the interconnection line structure that works as a terahertz antenna. We successfully identified the damaged MOSFETs by comparing the terahertz emission images between a normal chip and a defective one. This result suggests that the LTEM has the potential for a wide range of applications for the LSIC inspection in various stages of the manufacturing process.

The authors would like to acknowledge Tetsuya Sakai for preparing the defective MOSFET chip using FIB.

[1] B. Ferguson and X.-C. Zhang, Nat. Mater. **1**, 26 (2002).
[2] *Sensing with Terahertz Radiation*, edited by D. Mittleman (Springer, Berlin, 2002).
[3] T. Kiwa, M. Tonouchi, M. Yamashita, and K. Kawase, Opt. Lett. **28**, 2059 (2003).
[4] M. Yamashita, K. Kawase, C. Otani, K. Kiwa, and M. Tonouchi, Opt. Express **13**, 114 (2005).
[5] S. Kim, H. Murakami, and M. Tonouchi, IEEE J. Sel. Top. Quantum Electron. **14**, 498 (2008).
[6] K. Nikawa, Microelectron. Reliab. **37**, 1841 (1997).
[7] K. Nikawa, IEICE Trans. Electron. **E77-C**, 528 (1994).
[8] H. Fujioka and K. Nakame, IEICE Trans. Electron. **E77-C**, 535 (1994).
[9] K. Nikawa, in *Vortex Electronics and SQUIDs*, edited by T. Kobayashi, H. Hayakawa, and M. Tonouchi (Springer, Berlin, 2003), p. 224.